

Anyon delocalization transitions out of a disordered FQAH insulator

Zhengyan Darius Shi* and T. Senthil†

Department of Physics, Massachusetts Institute of Technology, Cambridge, Massachusetts 02139, USA

(Dated: June 4, 2025)

Motivated by the experimental discovery of the fractional quantum anomalous Hall (FQAH) effect, we develop a theory of doping-induced transitions out of the $\nu = 2/3$ lattice Jain state in the presence of quenched disorder. We show that disorder strongly affects the evolution into the conducting phases described in our previous work. The delocalization of charge $2/3$ anyons leads to a chiral topological superconductor through a direct second order transition for a smooth random potential with long wavelength modulations. The longitudinal resistance has a universal peak at the associated quantum critical point. For short wavelength disorder, this transition generically splits into three distinct ones with intermediate insulating topological phases. If instead, the charge $1/3$ anyon delocalizes, then at low doping the result is a Reentrant Integer Quantum Hall state with $\rho_{xy} = h/e^2$. At higher doping this undergoes a second transition to a Fermi liquid metal. We show that this framework provides a plausible explanation for the complex phase diagram recently observed in twisted MoTe_2 near $\nu = 2/3$ and discuss future experiments that can test our theory in more detail.

The discovery of zero-field fractional quantum anomalous Hall (FQAH) phases in twisted MoTe_2 ($t\text{MoTe}_2$) and rhombohedral graphene [1–6] opens up a new frontier in topological materials research. In common with conventional fractional quantum Hall (FQH) phases stabilized in a large external magnetic field [7], FQAH phases host anyon excitations with fractional charge and fractional statistics [8–12]. However, unlike in the large-field setting, anyons in FQAH phases are not confined to cyclotron orbits and carry a non-trivial band dispersion. Moreover, the two-dimensional Van der Waals materials that realize FQAH phases come with additional tuning knobs such as the displacement field, which allow for a continuous modulation of the anyon dispersion. This tunability enables us to explore the interplay between topology, electron kinetic energy and interactions.

The existence of non-trivial anyon dispersion has a profound impact on the fate of FQAH phases upon doping. In the large-field setting, anyons doped into the system carry no kinetic energy and become localized in the presence of disorder (see [13] and references therein). This mechanism explains the formation of quantum Hall plateaus which persist until the basic physics responsible for the emergence of anyons is destroyed. In contrast, the kinetic energy of anyons doped into an FQAH insulator competes with the disorder-induced tendency towards localization. This competition decreases the width of plateau regions and favors the formation of itinerant anyonic quantum phases upon exiting the plateau.

Recent theoretical works have explored the doped FQAH regime in an ideal limit with no disorder [14–16], finding a variety of interesting phases including topological superconductors and charge-ordered Fermi (and non-Fermi) liquids. Subsequently, an experiment in $t\text{MoTe}_2$ indeed finds a narrow plateau around the Jain state at

lattice filling $\nu = 2/3$ and a superconductor that emerges at $\nu > 2/3$ outside the plateau region [17]. On the opposite side $\nu < 2/3$, a reentrant integer quantum anomalous Hall (RIQAH) state apparently arises in between the plateaus surrounding $\nu = 2/3$ and $\nu = 3/5$. This rich phenomenology contrasts with the sequence of FQH plateau transitions that occur in the conventional quantum Hall setting within the same range of Landau level filling [7, 18].

Motivated by these experimental discoveries, we specialize to the lattice Jain state at filling $\nu = 2/3$ and study its evolution into the conducting states described in our previous work [14]. First, we study the chemical potential tuned FQAH-SC phase transition in both the clean and dirty limits. We also discuss a bandwidth tuned FQAH-SC transition at fixed lattice filling $\nu = 2/3$. Our analysis of the dirty limit shows that quenched disorder modifies the FQAH-SC evolution in striking ways that we elaborate on below. Second, we also analyse the chemical potential tuned evolution from the FQAH state to a charge-ordered Fermi liquid metal (also obtained in our previous work). In the presence of disorder, while the details of the evolution are complicated, the charge-ordered metal is replaced by an integer quantum Hall state in a portion of the phase diagram.

The main characters in our analysis are a pair of basic anyonic excitations of the Jain state, $a_{1/3}$ and $a_{2/3}$, which carry fractional charges $e/3$ and $2e/3$ respectively. The possible doping-induced phases as well as the universality class of phase transitions between them depend sensitively on the energetics of $a_{1/3}$ and $a_{2/3}$ in the undoped Jain state. When the energy gap of $a_{2/3}$ is smaller than twice the energy gap of $a_{1/3}$, the doped charges enter as a fluid of $a_{2/3}$ anyons¹. At low dopant density, disorder turns this fluid into a localized anyon glass. For

* zdshi@mit.edu

† senthil@mit.edu

¹ See Refs. [19, 20] for very recent calculations demonstrating bunching of anyons in a Landau level.

a smooth disorder potential with only long-wavelength modulations, increasing doping induces a direct continuous transition into a chiral topological superconductor with $c_- = -2$ (corresponding to four chiral Majorana edge modes). The longitudinal resistance has a universal peak of $\mathcal{O}(h/e^2)$ at the $T = 0$ quantum critical point, which is broadened at non-zero temperatures (see Fig. 2 and Fig. 3). With short-wavelength disorder (e.g. from point defects), a direct FQAH-SC transition is forbidden and the system instead passes through two intermediate phases with quantized electrical and thermal transport (see Fig. 4). The critical points between these phases have similarities with plateau transitions between FQH phases that we will comment on below.

When the energy gap of a localized $a_{2/3}$ anyon is larger than twice the energy gap of $a_{1/3}$, the dopant charges form a fluid of $a_{1/3}$ anyons instead. In this case, with both short and long-wavelength disorder, we argue that there is a direct transition from the anyon glass at low doping to an integer quantum Hall (IQH) state with $\sigma^{xy} = e^2/h$ at higher doping (see Fig. 5).

The theory developed above applies to any doped lattice $\nu = 2/3$ Jain state. The main input from microscopics is the relative gap sizes of distinct anyons which determine whether $a_{1/3}$ or $a_{2/3}$ is doped into the system. Armed with our theoretical analysis, we discuss the observation of SC and RIQAH states proximate to the $\nu = 2/3$ FQAH state in $t\text{MoTe}_2$. We propose an interpretation of the $t\text{MoTe}_2$ phase diagram in Ref. [17], in which doping towards $|\nu| > 2/3$ induces a fluid of $a_{2/3}$ anyons, while doping towards $|\nu| < 2/3$ induces a fluid of $\bar{a}_{1/3}$ anyonic holes. This asymmetry in the particle and hole excitation spectrum leads to an asymmetric phase diagram in which $\nu > 2/3$ realizes a superconductor while $\nu < 2/3$ realizes a localized IQH state.

Low energy theory near $\nu = 2/3$: Following Ref. [14], we describe the Jain state at lattice filling $\nu = 2/3$ through a parton construction in which the microscopic electron c is fractionalized as $c = f_1 f_2 f_3$. The low energy Lagrangian takes the form

$$L = L[f_1, a] + L[f_2, b - a] + L[f_3, A - b], \quad (1)$$

where a, b are emergent $U(1)$ gauge fields introduced to remove the redundancy in the parton decomposition. The equations of motion for a_t and b_t enforce the constraint $\rho_1 = \rho_2 = \rho_3 = \rho_c$, where ρ_i/ρ_c is the charge density of f_i/c respectively. In units where the lattice constant is set to 1, we can consider a uniform mean-field ansatz in which

$$\frac{\langle \nabla \times \mathbf{a} \rangle}{2\pi} = -\frac{1}{3}, \quad \frac{\langle \nabla \times \mathbf{b} \rangle}{2\pi} = \frac{1}{3}. \quad (2)$$

This choice ensures that the flux seen by f_i is commensurate with its lattice filling $\nu_i = 2/3$. Therefore, each f_i can form a Chern insulator with total Chern number C_i determined by the detailed band structure. To construct the Jain state at $\nu = 2/3$, the unique Chern number assignment (up to permutations) is $C_1 = -2, C_2 = C_3 =$

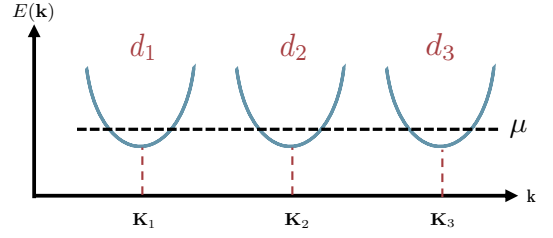


FIG. 1. A schematic depiction of the continuum fields d_I that create excitations of the f_3 band near its minima $\mathbf{K}_1, \mathbf{K}_2, \mathbf{K}_3$. When μ is above the band bottom, the d_I particles see an emergent magnetic field proportional to their density, which is not shown in the figure.

1 [14]. With this choice, we can integrate out the gapped partons f_i as well as the gauge field a to obtain²

$$L = \frac{3}{4\pi} bdb - \frac{1}{2\pi} bdA + \frac{1}{4\pi} AdA + 2CS_g. \quad (3)$$

Upon doping away from $\nu = 2/3$, the excess charges form a dilute itinerant anyon fluid. The key observation in Ref. [14] is that the fate of this anyon fluid at zero temperature depends on the energetics of different anyons in the parent FQAH insulator. In the parton description, the $a_{1/3}$ anyon is sourced by f_1 (the zero-field analogue of the composite fermion) and the $a_{2/3}$ anyon is sourced by f_2 or f_3 . Therefore, the question of which anyon gets doped into the system translates to the question of which parton band is closest to the chemical potential. We now consider both possibilities (doping in $a_{2/3}$ or $a_{1/3}$) and analyze the evolution out of the FQAH phase with and without quenched disorder.

Doping the $a_{2/3}$ anyon: clean limit Let us first study the situation in which the $a_{2/3}$ anyon is doped into the system. In the absence of disorder, the phase transition out of the FQAH state occurs (within the parton description) when the chemical potential μ touches the minima of the unfilled f_3 band. Lattice translations T_x, T_y act projectively on f_3 as it sees $2\pi/3$ flux per plaquette. Thus f_3 carries well-defined crystal momenta in a three-fold reduced Brillouin zone, and its band structure has three degenerate minima at $\mathbf{K}_1, \mathbf{K}_2, \mathbf{K}_3$ such that $|\mathbf{K}_I - \mathbf{K}_J|$ is a multiple of $2\pi/3$. Near the critical point, it is convenient to introduce three species of continuum fermionic fields d_I that create f_3 excitations near \mathbf{K}_I and transform projectively under lattice translation (see Fig. 1 for an illustration)

$$T_x : d_I \rightarrow d_{I+1}, \quad T_y : d_I \rightarrow e^{2\pi i I/3} d_I. \quad (4)$$

² We include in the continuum effective theory a coupling to a background space-time metric g . The gravitational Chern-Simons term $2CS_g$ enables us to keep track of the thermal Hall conductance of various phases.

In terms of these fields, the low energy effective Lagrangian takes the form

$$L_{\text{clean}, a_{2/3}} = \sum_{I=1}^3 d_I^\dagger \left[i\partial_t + \mu + A_t - b_t - \frac{(i\nabla + \mathbf{A} - \mathbf{b})^2}{2m} \right] d_I \quad (5) \\ + L_{\text{int}}[d_I] + \frac{3}{4\pi} bdb - \frac{1}{2\pi} bdA + \frac{1}{4\pi} AdA + 2\text{CS}_g,$$

where m is the effective mass of f_3 near the band minima and L_{int} includes repulsive interactions between the d_I fermions. When $\mu < 0$, the d_I fermions are gapped and we recover the Jain state described by (3). When $\mu > 0$, the equations of motion for b_t enforce the constraint $\sum_{I=1}^3 \rho_I = \frac{3}{2\pi} \langle \nabla \times \mathbf{b} \rangle$. Since d_I feels an effective magnetic field $-\nabla \times \mathbf{b}$, this constraint implies that each d_I is at Landau level filling -1 and forms an IQH state. Integrating out the filled Landau levels of d_I gives the chiral topological superconductor

$$L_{\text{SC}} = \frac{2}{2\pi} bdA - \frac{2}{4\pi} AdA - 4\text{CS}_g. \quad (6)$$

At the critical point $\mu = 0$, the mean-field propagator for d_I takes the simple form

$$G_{IJ}^{(d)}(\mathbf{k}, i\omega) = \frac{\delta_{IJ}}{i\omega - k^2/(2m)}. \quad (7)$$

As a result, the dynamical critical exponent is $z = 2$ and the correlation length exponent is $\bar{\nu} = 1/2$. A short-range interaction of the form $V_{IJ}\rho_I\rho_J$ is marginal at tree level. Following the same calculation as in the Bose-Hubbard model [21], we can show that V_{IJ} is marginally irrelevant and can be neglected at the IR fixed point.

The interaction between d_I and the gauge field b is also marginal by power counting. Nevertheless, we can argue that the gauge and matter sectors decouple at zero temperature. The physical reason is that the dispersion of d_I contains a “particle” branch above μ but no hole branch below μ . This means that the ground state contains no occupied fermionic modes and particle-hole excitations do not exist at zero temperature. Since the gauge field b couples to particle-hole excitations, this observation immediately implies the decoupling between matter and gauge sectors at $T = 0$. On a more technical level, this is equivalent to the statement that poles of $G_{IJ}^{(d)}(\mathbf{k}, i\omega)$ in the complex ω -plane always satisfy $\text{Im}[\omega] < 0$. This pole structure guarantees that all loop corrections to the gauge field self-energy vanish identically.

Doping the $a_{2/3}$ anyon: dirty limit For real experimental systems, quenched disorder is ubiquitous and modifies the above picture dramatically. The most relevant form of disorder near the phase transition is a generalized random potential that breaks the lattice translation symmetry completely

$$L_{\text{dis}} = W_{IJ}(\mathbf{r}) d_I^\dagger(\mathbf{r}, t) d_J(\mathbf{r}, t) + W_b(\mathbf{r}) \frac{\nabla \times \mathbf{b}(\mathbf{r}, t)}{2\pi}. \quad (8)$$

When μ is positive but small, each of the d_I fermions wants to form an IQH state with a small energy gap $\omega_c(\delta) \sim \delta/m$, where $\delta \ll 1$ is the density of d_I . Let \bar{W}_{IJ}, \bar{W}_b characterize the strength of the disorder potentials $W_{IJ}(\mathbf{r}), W_b(\mathbf{r})$. If $\omega_c(\delta) \ll \bar{W}_{IJ}, \bar{W}_b$, the mean-field quantum Hall state for d_I is replaced by a localized state with vanishing σ^{xx} and σ^{xy} . Gauge fluctuations turn this mean-field state into a localized “anyon glass”, leading to a plateau surrounding the $\nu = 2/3$ state with quantized $\sigma^{xy} = 2e^2/3h$. In the opposite limit where $\omega_c(\delta) \gg \bar{W}_{IJ}, \bar{W}_b$, the disorder potential is a weak perturbation to the mean-field IQH state of d_I and we recover a disordered superconductor.

The evolution from the anyon glass to the superconductor depends on the spatial profile of the disorder potentials. When $W_{IJ}(\mathbf{r})/W_b(\mathbf{r})$ is a smooth potential with only long-wavelength modulations, we can truncate the Fourier modes $W_{IJ}(\mathbf{q})/W_b(\mathbf{q})$ at some small momentum cutoff $q_{\text{max}} \ll 1$ (in units where the lattice spacing is 1). In the low energy effective theory, this means that disorder potentials that transform under the action of lattice translations should be excluded. From (4), it is clear that $d_I^\dagger T_{IJ} d_J$, with T_{IJ} any $SU(3)$ matrix, transforms non-trivially under T_x and/or T_y . Therefore, the only terms compatible with smooth disorder take the form

$$L_{\text{dis,smooth}} = W_d(\mathbf{r}) \sum_{I=1}^3 d_I^\dagger d_I + W_b(\mathbf{r}) \frac{\nabla \times \mathbf{b}(\mathbf{r})}{2\pi}. \quad (9)$$

When $L_{\text{dis,smooth}}$ is added to the critical theory, the combined Lagrangian enjoys an emergent $SU(3)$ symmetry³ that rotates the fermionic fields d_I . As we increase the dopant density δ , there is a critical δ_c at which d_I goes through an $SU(3)$ -symmetric plateau transition with a jump in the Hall conductance $\Delta\sigma_d^{xy} = -3e^2/h$. With gauge fluctuations, this turns into a direct transition from the anyon glass (with quantized $\sigma^{xy} = 2e^2/3h$) to the topological superconductor described by (6).

While the precise critical exponents of this transition are difficult to access analytically, there are a number of qualitative features that can be immediately deduced. At the single particle level, the d_I fermions are gapless but not gauge-invariant. The gauge-invariant electron operator c can be constructed by combining d_I with the gapped partons f_1 and f_2 . Therefore, the microscopic electron remains gapped across the phase transition and single particle tunneling sees no spectral weight at frequencies below the f_1/f_2 gap.

Going into the superfluid phase, the critical theory also determines the scaling of the superfluid stiffness ρ_s with the tuning parameter $|\mu - \mu_c|$

$$\rho_s \sim \xi^{-z} \sim |\mu - \mu_c|^{\bar{\nu}z}. \quad (10)$$

³ More precisely, the symmetry is $PSU(3) = SU(3)/\mathbb{Z}_3$.

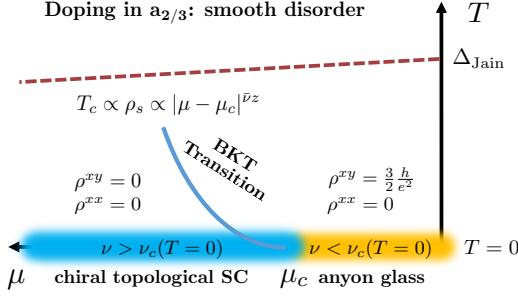


FIG. 2. Onset of T_c and ρ_s as a function of $\mu - \mu_c$ across the FQAH-SC phase transition with smooth disorder. In this phase diagram, we assume $\mu - \mu_c$ is small enough that the Jain gap Δ_{Jain} remains much higher than T_c . Importantly, since $\bar{\nu}z \geq 2$, $T_c(\mu)$ and $\rho_s(\mu)$ have zero slope near $\mu = \mu_c$.

Standard arguments [21, 22] for disordered superfluid-insulator transitions apply to the present FQAH-SC transition as well. With short-range interactions, both phases as well as the critical point are expected to be compressible and this implies an exact dynamical critical exponent $z = 2$. With Coulomb interactions, z is modified to 1. Moreover, by the Harris-Chayes bound [23, 24], the correlation length exponent $\bar{\nu}$ satisfies the inequality $\bar{\nu} \geq 1$ in two dimensions. As a result, $\bar{\nu}z \geq 2$ and $\rho_s(\mu)$ has zero slope at $\mu = \mu_c$. At a non-zero temperature, the superconducting state will be stable up to a Berezinsky-Kosterlitz-Thouless (BKT) transition temperature T_c which will go to zero as the quantum critical point is approached in the same way as the ground state ρ_s . The onset of ρ_s and T_c as a function of $|\mu - \mu_c|$ is very slow, as illustrated in Fig. 2.

In terms of transport, general scaling arguments imply that the critical theory has a universal non-zero resistivity tensor ρ_c with both longitudinal and Hall components of $\mathcal{O}(h/e^2)$ [21, 25–27]. This may be approximately related to the conductivity tensor σ_d of d_I through the Ioffe-Larkin rule

$$\rho_c = \begin{pmatrix} 0 & -1/2 \\ 1/2 & 0 \end{pmatrix} + \left[\begin{pmatrix} 0 & 1 \\ -1 & 0 \end{pmatrix} + \sigma_d \right]^{-1}. \quad (11)$$

Computing the inverse explicitly gives

$$\begin{aligned} \rho_c^{xx} &= \frac{\sigma_d^{xx}}{(\sigma_d^{xx})^2 + (1 + \sigma_d^{xy})^2}, \\ \rho_c^{yx} &= \frac{1}{2} + \frac{1 + \sigma_d^{xy}}{(\sigma_d^{xx})^2 + (1 + \sigma_d^{xy})^2}. \end{aligned} \quad (12)$$

Thus the critical point is signaled by a universal peak in ρ^{xx} . At $T > 0$, the peak is broadened by thermal fluctuations, with a width that scales as $T^{1/(\bar{\nu}z)}$. This phenomenology is summarized in Fig. 3.

The story is drastically different when the microscopic disorder potentials $W_{IJ}(\mathbf{r})$ and $W_b(\mathbf{r})$ have significant variations at the lattice scale. In this case, all components of W_{IJ} must be included and the emergent $SU(3)$

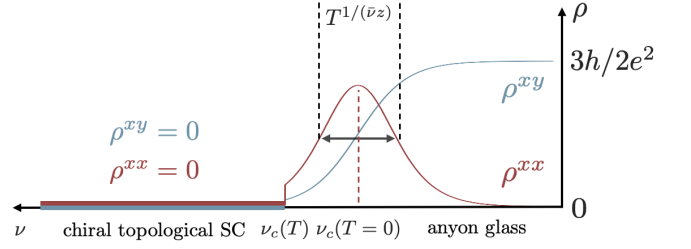


FIG. 3. Evolution of ρ upon doping $a_{2/3}$ at fixed $T > 0$ with smooth disorder. To match the experimental convention, our plot shows ν increasing towards the left. $\nu_c(T = 0)$ marks the $T = 0$ critical point with universal transport and $\nu_c(T)$ defines the BKT transition curve at $T > 0$. When $\nu > \nu_c(T)$, dissipationless superflow sets in and ρ vanishes abruptly.

symmetry in the clean Lagrangian is completely broken. As δ increases, the evolution from $\sigma_d^{xy} = 0$ to $\sigma_d^{xy} = -3$ passes through three separate phase transitions, as σ_d^{xy} can only jump by ± 1 at each critical point. When $\sigma_d^{xy} = -1$, the effective Lagrangian reduces to

$$L[\sigma_d^{xy} = -1] = \frac{2}{4\pi} bdb, \quad (13)$$

which describes a localized insulator that coexists with a neutral $U(1)_{-2}$ topological order. This phase is indistinguishable from a trivial localized insulator in electric transport, but has a single neutral chiral edge mode with $\kappa_{xy} = -2\kappa_Q$ that can potentially be detected in thermal Hall measurements.⁴ When $\sigma_d^{xy} = -2$, the effective Lagrangian becomes

$$L[\sigma_d^{xy} = -2] = \frac{1}{4\pi} bdb + \frac{1}{2\pi} b dA - \frac{1}{4\pi} A dA - 2CS_g. \quad (14)$$

Integrating out b simplifies this Lagrangian further to

$$L[\sigma_d^{xy} = -2] = -\frac{2}{4\pi} A dA - 4CS_g, \quad (15)$$

which describes an IQH state with Hall conductance $\sigma^{xy} = -2$. Putting all of these results together, we arrive at the phase diagram in Fig. 4, where each critical point is associated with a universal $\mathcal{O}(h/e^2)$ resistivity tensor. At $T > 0$, the width of the transition region scales as $T^{1/(\bar{\nu}z)}$, while the critical resistivity is independent of T . Importantly, although the three critical points involve the same jump in σ_d^{xy} at the mean field level, they differ in the structure of gauge interactions and could have distinct critical exponents. If we decrease the disorder strength at fixed T , the range of δ over which the three transitions occur shrinks and the peaks eventually merge into a smoother evolution of ρ^{xx} and ρ^{yx} .

⁴ This state can also be obtained by doping the CDW* state with neutral $U(1)_{-2}$ topological order at $\nu = 2/3$ which is accessible from the Jain state through a bandwidth-tuned transition [28].

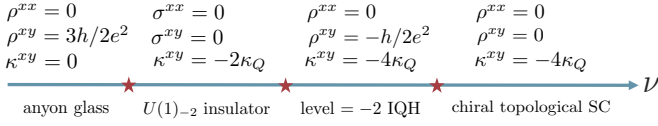


FIG. 4. With short-wavelength disorder, the FQAH-SC evolution passes through three intermediate phases with quantized ρ and κ^{xy} . In the phase diagram above, $U(1)_{-2}$ is a neutral topological order and κ_Q denotes the thermal Hall quantum corresponding to a single Majorana edge mode.

Doping the $a_{1/3}$ anyon; We now turn to the second possibility, in which the doped anyon is $a_{1/3}$ and the f_1 band is closest to the chemical potential. In the clean limit, we again introduce three species of d_I that create excitations of f_1 near its band minima at \mathbf{K}_I such that d_I transforms projectively under T_x, T_y as in (4). The low energy effective Lagrangian then takes the form

$$L_{\text{clean}, a_{1/3}} = \sum_{I=1}^3 d_I^\dagger \left[i\partial_t + \mu + a_t - \frac{(i\nabla + \mathbf{a})^2}{2m} \right] d_I + L_{\text{int}}[d_I] \quad (16)$$

$$- \frac{1}{4\pi} ada + \frac{2}{4\pi} bdb + \frac{1}{4\pi} AdA - \frac{1}{2\pi} bd(A + a),$$

where m now denotes the effective mass of f_1 near the band minima. When $\mu < 0$, d_I is gapped and we recover the Jain state. When $\mu > 0$, the equations of motion for a_t and b_t enforce the constraint $\sum_I \rho_I = \frac{3}{2} \frac{1}{2\pi} \langle \nabla \times \mathbf{a} \rangle$. At the mean-field level, each d_I feels an effective magnetic field $\nabla \times \mathbf{a}$ and is at Landau level filling 1/2. Therefore, the three species of d_I form three pockets of composite Fermi liquids coupled to a common fluctuating gauge field a . The analysis in Ref. [14] shows that gauge fluctuations induce interpocket pairing between two out of the three pockets and confine all the fluctuating gauge fields. The resulting ground state is a charge-ordered Fermi liquid coexisting with a background IQH state

$$L_{\text{FL}} = L_{\text{FL}}[c, A] + \frac{1}{4\pi} AdA + 2CS_g. \quad (17)$$

The clean critical theory is identical to the clean FQAH-SC transition at the mean field level and the argument for decoupling between gauge and matter sectors still holds at $T = 0$. At $T > 0$, this transition differs from the FQAH-SC transition since the relevant gauge fields have different Chern-Simons terms. A quantitative understanding of these finite-temperature properties is an interesting target for future studies.

The story has an interesting twist when we include quenched disorder. With long-wavelength disorder, the random potential Lagrangian still takes the $SU(3)$ symmetric form in (9). At low doping, the resulting state is an anyon glass (with quantized $\sigma^{xy} = 2e^2/3h$) made of $a_{1/3}$ instead of $a_{2/3}$. Unlike in the FQAH-SC case, the mean-field transition is not an IQH plateau transition of d_I . Instead, it describes the sudden creation of

three composite fermion pockets out of a localized insulator, about which very little is understood. Moreover, on the other side of the phase transition, the Fermi liquid with period-3 charge order predicted by the clean theory will not be stable to localization effects at low doping density. In the resulting state if this localization occurs, the $L_{\text{FL}}[c, A]$ part of (17) becomes a Fermi glass and the theory describes an IQH state with quantized $\sigma^{xx} = 0$ and $\sigma^{xy} = e^2/h$. Further in the approximation that the smooth disorder potential does not couple linearly to the CDW order parameter, the charge order will survive in this IQH state.

With short-wavelength disorder, the random potential breaks the $SU(3)$ symmetry. At finite doping the charge order of the doped Fermi liquid will be unstable to disorder. As before at low doping densities the Fermi liquid will again be unstable to localization. The integer quantum Hall effect of the clean CDW metal will survive. Let us now consider the evolution from the FQAH to this IQH phase. The individual filling factors of d_I are no longer meaningful and we can regard d_I as a three-component fermion at total Landau level filling 3/2. At low doping, d_I forms a localized insulator and we again have an anyon glass of $a_{1/3}$. This of course is part of the FQAH plateau. Upon increasing the doping, it is natural to encounter a plateau transition in which the total Hall conductance of the d_I sector jumps by 1. When this occurs, the effective Lagrangian becomes

$$L = \frac{2}{4\pi} bdb + \frac{1}{4\pi} AdA - \frac{1}{2\pi} bd(A + a) + 2CS_g. \quad (18)$$

Integrating out a sets $b = 0$ and gives

$$L[\sigma_d^{xy} = 1] = \frac{1}{4\pi} AdA + 2CS_g, \quad (19)$$

which just describes an IQH state coexisting with a localized Fermi glass. As argued above, this is exactly the fate of the clean CDW metal (+IQH) at low charge densities in the presence of short wavelength disorder.

Therefore, the most natural state that arises from doping in $a_{1/3}$ is an IQH state with quantized $\sigma^{xy} = e^2/h$, although the nature of the transition from the Jain state to this IQH state could depend on the type of quenched disorder. A schematic transport plot is shown in Fig. 5.

Bandwidth-tuned FQAH-SC transition: We now briefly consider the possibility that the FQAH state can be tuned to a SC at fixed lattice filling $\nu = 2/3$ by varying the bandwidth (e.g. with a displacement field) in the clean limit. To that end, we begin with the parton description of the FQAH state in terms of f_i for $i = 1, 2, 3$ each filling a Chern band with Chern numbers C_i such that $C_1 = -2, C_2 = C_3 = 1$. We consider a phase transition at fixed filling where the Chern number of f_3 changes away from 1 (through band inversion) while the f_1, f_2 Chern numbers stay fixed. As we discussed, the projective action of translation symmetry implies that there are three inequivalent points in the Brillouin zone that are degenerate in energy. Consequently, the band

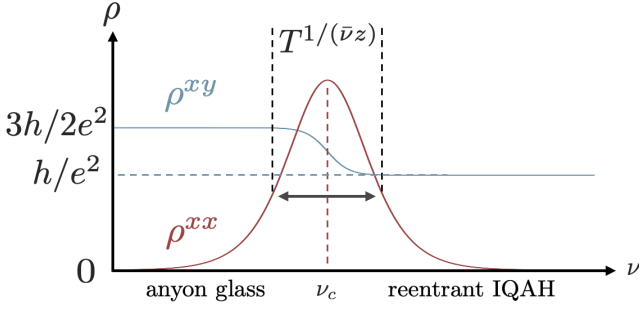


FIG. 5. Evolution of ρ^{xx} and ρ^{xy} upon doping the $a_{1/3}$ anyon. At $\nu > \nu_c$, the inclusion of disorder turns the charge-ordered Fermi liquid in the clean model into a reentrant IQAH state.

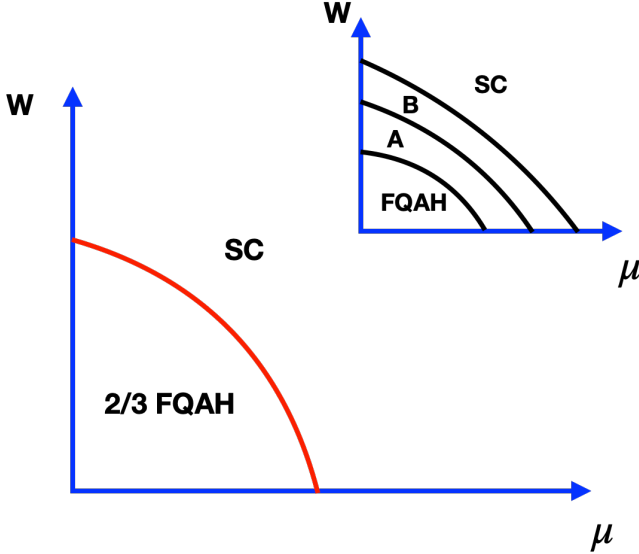


FIG. 6. Schematic phase diagram showing the $2/3$ Jain FQAH and chiral topological SC in the bandwidth(W) -chemical potential(μ) plane. In a clean system, the phase transition at fixed lattice filling is in a different universality class described by the QED₃-Chern Simons theory of Eqn. 22. Inset: Dirty limit (with short wavelength disorder): The transition goes through two intermediate phases; phase (A) is an insulator with a neutral topological order and (B) is an integer quantum Hall insulator.

touching happens simultaneously at these three points, each described by a massless Dirac fermion. The f_3 Chern number can therefore only jump by multiples of 3 so long as the lattice translation symmetry is preserved.

Consider now a phase where the Chern number of f_3 has changed from its original value $C_3 = 1$ in the FQAH phase to $C_3 = -2$. The low energy effective theory of the resulting phase is

$$L = \frac{2}{4\pi}bdb - \frac{2}{4\pi}(A-b)d(A-b) - 4CS_g \quad (20)$$

$$= \frac{2}{2\pi}bdA - \frac{2}{4\pi}AdA - 4CS_g. \quad (21)$$

Integrating out b , we see that we get a charge-2 superconductor with a chiral central charge $c_- = -2$, which is smoothly connected to the one obtained by doping the FQAH state with the $a_{2/3}$ anyon (6). At the phase transition, the critical Lagrangian takes the form

$$L_{\text{Dirac}} = \sum_{I=1}^3 d_I^\dagger (i\not{\partial} + \not{A} - \not{b}) d_I \quad (22)$$

$$+ \frac{3}{4\pi}bdb - \frac{1}{2\pi}bdA + \frac{1}{4\pi}AdA + 2CS_g.$$

This is a QED₃ theory with $N_f = 3$ massless Dirac fermions (representing the 3 band touching points of f_3) coupled to an emergent gauge field $A - b$. As a relativistic theory, it has $z = 1$ and power-law correlations in the CDW order parameters $d_I^\dagger T_{IJ} d_J$ (with T_{IJ} an $SU(3)$ matrix). Its properties are similar to an analogous transition between the bosonic $\nu = 1/2$ Laughlin and superfluid states, which has $N_f = 2$ and distinct Chern-Simons terms. In Appendix A, we show that a useful perspective on this transition as well as the doping-induced FQAH-SC transition can be obtained by relating them to transitions out of the bosonic Jain state at $\nu = 2/3$.

A schematic phase diagram in the full bandwidth-chemical potential plane is shown in Fig. 6.

Application to doped $t\text{MoTe}_2$: A recent experimental study [17] of a high quality hole-doped $t\text{MoTe}_2$ device explored the phase diagram in the vicinity of the prominent $\nu = 2/3$ FQAH state. In a small range of displacement field near zero, a SC state is found at fillings $0.71 \lesssim \nu \lesssim 0.76$. This SC is separated from the FQAH state by a region where the longitudinal resistance ρ^{xx} peaks with a peak height of order h/e^2 (in the range $10 - 15 \text{ k}\Omega$). On the other side with ν just smaller than $2/3$, an integer quantum Hall response is found (dubbed the Reentrant Integer Quantum Anomalous Hall (RIQAH) state) in ρ^{xy} and ρ^{xx} . This too is separated from the FQAH state by a peak in ρ^{xx} . Caution is however needed in interpreting the RIQAH response: a plot of the Streda slope in this state yields a σ^{xy} closer to $2/3$ than to 1. This discrepancy may indicate issues [29–33] with edge equilibration in the multi-component edge expected for the $2/3$ FQAH state which could lead to a spurious value of the measured ρ^{xy} . An RIQAH response is also seen at higher displacement field for $\nu \gtrsim 2/3$ (with the same concerns as above with the Streda slope).

It is important for future experiments to resolve this discrepancy between transport and the Streda slopes, and to have further confirmation of the superconducting state. We have argued that it is reasonable *theoretically* to expect both superconductivity and an RIQAH state in proximity to the $2/3$ FQAH plateau. Let us therefore examine the existing experimental data in light of our theory.

There are several preliminary questions that need to be settled before interpreting these observations in terms of the theory developed in this paper. For the observed superconductor, it is important to know if the mobile

charge carrier density is “small” (corresponding to filling $2/3 - \nu$, the deviation from $2/3$) or if it is “large” (corresponding to filling $1 - \nu$). If the former, then a description as a doped FQAH state - which will naturally involve doped anyons - is the right framework. If the latter, then it is appropriate to think of the SC as developing out of a normal state that is separated from the FQAH state by a strong first order transition, and the theory described in this paper is not directly pertinent. The existing data reveals a sign change of the Hall effect at high fields $B \gtrsim 2$ T near $\nu \approx 0.75$ at $D = 0$ below which SC first develops. This could be consistent with a ‘large’ to ‘small’ carrier density change. More detailed studies - as sketched in Appendix B - are needed to determine whether the carrier density truly decreases towards zero as ν approaches $2/3$.

Assuming that the doped FQAH framework is applicable, the theory developed so far provides a possible explanation of these observations. At displacement field $D = 0$ and $\nu = 2/3$, we propose that the anyon energetics of the Jain state has a particle-hole asymmetry, such that doping towards $\nu > 2/3$ induces a fluid of $a_{2/3}$, while doping towards $\nu < 2/3$ induces a fluid of $a_{1/3}$. This translates to a parabolic band structure where the conduction (valence) band closest to the chemical potential is associated with f_3 (f_1). With long-wavelength disorder⁵, there is a narrow plateau with quantized $\sigma^{xy} = 2e^2/3h$ for $\nu \in [\nu_1, \nu_2]$ with $\nu_1 < 2/3 < \nu_2$. Doping beyond the plateau, our theory predicts a topological superconductor at $\nu > \nu_2$ and an RIQAH state at $\nu < \nu_1$. While all three phases have $\rho^{xx} = 0$, the transitions between them feature $\mathcal{O}(h/e^2)$ peaks in ρ^{xx} , broadly consistent with the experimental observations in Ref. [17]. In the $T \rightarrow 0$ limit, the height of the ρ^{xx} peak at either transition is expected to saturate to a non-zero value while the width should decrease to zero as we described earlier. It would be interesting for future experiments to clarify these features of the resistance peaks.

An important future direction is a microscopic calculation of anyon energetics within models of $t\text{MoTe}_2$. It will be interesting to see if ‘anyon bunching’ of the kind reported in very recent calculations[19, 20] of Landau level

FQH states happens in FQAH states found in models of $t\text{MoTe}_2$. However, even without numerics, existing data already provide some qualitative guidance. Given the sequence of Jain states observed near $\nu = 1/2$, it is natural to expect that the $\nu < 2/3$ side fits into the standard “composite fermion” framework [35]. Since f_1 is the zero-field analogue of the composite fermion (see Ref. [14, 36, 37]), it is reasonable to associate the nearest valence band with f_1 . On the other hand, for $\nu > 2/3$, there is no a priori reason for the composite fermion framework to apply. Thus, our proposal of f_3 being the nearest conduction band becomes more plausible.

Tuning away from $D = 0$ modifies the anyon dispersion at $\nu = 2/3$. If there exists a critical D_c such that the nearest conduction band switches from f_3 to f_1 for $D > D_c$, then doping induces a fluid of $a_{1/3}$ anyons for both $\nu > 2/3$ and $\nu < 2/3$. This switching effect provides a potential explanation for the pair of RIQAH states observed in a range of displacement fields $15 \lesssim D \lesssim 30$ nV/nm on both sides of the FQAH plateau [17].

It will also be important to have an experimental determination of the charge of the delocalizing anyon. This may be easier in the FQAH/anyon glass phase prior to the delocalization transition. Standard measurements[38–40] of the anyon charge successfully used in ordinary FQH systems are of course worth exploring in the FQAH context. An indirect route, specific to the lattice setting, is to look for local charge density modulations that are expected[41] to appear around each localized anyon (with short wavelength disorder) in a halo region at low dopant density. This is due to the close competition between FQAH and Charge Density Wave (CDW) phases in a clean system. Around each anyon, the FQAH is locally suppressed enabling the CDW to rear its head. These modulations may be measurable in Scanning Tunneling Microscopy experiments and their density can potentially yield the anyon charge[41].

Note added—We are coordinating submission with Ref. [42], where closely related results were obtained.

Acknowledgements: We thank Tonghang Han, Pavel Nosov, and Heonjoon Park for discussions. ZDS and TS are supported by NSF grant DMR-2206305.

[1] H. Park, J. Cai, E. Anderson, Y. Zhang, J. Zhu, X. Liu, C. Wang, W. Holtzmann, C. Hu, Z. Liu, T. Taniguchi, K. Watanabe, J.-H. Chu, T. Cao, L. Fu, W. Yao, C.-Z. Chang, D. Cobden, D. Xiao, and X. Xu, Observation of fractionally quantized anomalous Hall effect, *Nature* (London) **622**, 74 (2023), arXiv:2308.02657 [cond-mat.mes-hall].

[2] Y. Zeng, Z. Xia, K. Kang, J. Zhu, P. Knüppel, C. Vaswani, K. Watanabe, T. Taniguchi, K. F. Mak, and J. Shan, Integer and fractional Chern insulators in twisted bilayer MoTe_2 , *arXiv e-prints*, arXiv:2305.00973 (2023), arXiv:2305.00973 [cond-mat.mes-hall].

[3] J. Cai, E. Anderson, C. Wang, X. Zhang, X. Liu, W. Holtzmann, Y. Zhang, F. Fan, T. Taniguchi, K. Watanabe, Y. Ran, T. Cao, L. Fu, D. Xiao, W. Yao, and X. Xu, Signatures of fractional quantum anomalous Hall states in twisted MoTe_2 , *Nature* (London) **622**, 63 (2023), arXiv:2304.08470 [cond-mat.mes-hall].

⁵ In high quality $t\text{MoTe}_2$ devices, the density of charged point defects (which generate short-wavelength disorder) is about a factor of 100 smaller than the electron density [34]. It is thus plausible that other sources of disorder (such as a random twist angle), which are only modulated at long wavelengths, play a dominant role.

- [4] F. Xu, Z. Sun, T. Jia, C. Liu, C. Xu, C. Li, Y. Gu, K. Watanabe, T. Taniguchi, B. Tong, J. Jia, Z. Shi, S. Jiang, Y. Zhang, X. Liu, and T. Li, Observation of Integer and Fractional Quantum Anomalous Hall Effects in Twisted Bilayer MoTe₂, *Physical Review X* **13**, 031037 (2023), [arXiv:2308.06177 \[cond-mat.mes-hall\]](#).
- [5] Z. Lu, T. Han, Y. Yao, A. P. Reddy, J. Yang, J. Seo, K. Watanabe, T. Taniguchi, L. Fu, and L. Ju, Fractional quantum anomalous Hall effect in multilayer graphene, *Nature (London)* **626**, 759 (2024), [arXiv:2309.17436 \[cond-mat.mes-hall\]](#).
- [6] Z. Lu, T. Han, Y. Yao, Z. Hadjri, J. Yang, J. Seo, L. Shi, S. Ye, K. Watanabe, T. Taniguchi, and L. Ju, Extended quantum anomalous Hall states in graphene/hBN moiré superlattices, *Nature (London)* **637**, 1090 (2025), [arXiv:2408.10203 \[cond-mat.mes-hall\]](#).
- [7] H. L. Stormer, D. C. Tsui, and A. C. Gossard, The fractional quantum hall effect, *Rev. Mod. Phys.* **71**, S298 (1999).
- [8] J. M. Leinaas and J. Myrheim, On the theory of identical particles, *Nuovo Cim. B* **37**, 1 (1977).
- [9] F. Wilczek, Magnetic flux, angular momentum, and statistics, *Phys. Rev. Lett.* **48**, 1144 (1982).
- [10] F. Wilczek, Quantum mechanics of fractional-spin particles, *Phys. Rev. Lett.* **49**, 957 (1982).
- [11] R. B. Laughlin, Anomalous quantum hall effect: An incompressible quantum fluid with fractionally charged excitations, *Phys. Rev. Lett.* **50**, 1395 (1983).
- [12] B. I. Halperin, Statistics of quasiparticles and the hierarchy of fractional quantized hall states, *Phys. Rev. Lett.* **52**, 1583 (1984).
- [13] B. Huckestein, Scaling theory of the integer quantum hall effect, *Rev. Mod. Phys.* **67**, 357 (1995).
- [14] Z. Darius Shi and T. Senthil, Doping a fractional quantum anomalous Hall insulator, [arXiv e-prints](#), [arXiv:2409.20567 \(2024\)](#), [arXiv:2409.20567 \[cond-mat.str-el\]](#).
- [15] M. Kim, A. Timmel, L. Ju, and X.-G. Wen, Topological chiral superconductivity (2024), [arXiv:2409.18067 \[cond-mat.str-el\]](#).
- [16] Z. Darius Shi, C. Zhang, and T. Senthil, Doping lattice non-abelian quantum Hall states, [arXiv e-prints](#), [arXiv:2505.02893 \(2025\)](#), [arXiv:2505.02893 \[cond-mat.str-el\]](#).
- [17] F. Xu, Z. Sun, J. Li, C. Zheng, C. Xu, J. Gao, T. Jia, K. Watanabe, T. Taniguchi, B. Tong, L. Lu, J. Jia, Z. Shi, S. Jiang, Y. Zhang, Y. Zhang, S. Lei, X. Liu, and T. Li, Signatures of unconventional superconductivity near reentrant and fractional quantum anomalous Hall insulators, [arXiv e-prints](#), [arXiv:2504.06972 \(2025\)](#), [arXiv:2504.06972 \[cond-mat.mes-hall\]](#).
- [18] R. Willett, J. P. Eisenstein, H. L. Stormer, A. C. Gossard, and D. C. Tsui, Observation of an even-denominator quantum number in the fractional quantum Hall effect, *Phys. Rev. Lett.* **59**, 1776 (1987).
- [19] Q. Xu, G. Ji, Y. Wang, H. Quang Trung, and B. Yang, Dynamics of Clusters of Anyons in Fractional Quantum Hall Fluids, [arXiv e-prints](#), [arXiv:2505.20257 \(2025\)](#), [arXiv:2505.20257 \[cond-mat.str-el\]](#).
- [20] M. Gattu and J. K. Jain, Molecular anyons in fractional quantum hall effect (2025), [arXiv:2505.22782 \[cond-mat.str-el\]](#).
- [21] M. P. A. Fisher, P. B. Weichman, G. Grinstein, and D. S. Fisher, Boson localization and the superfluid-insulator transition, *Phys. Rev. B* **40**, 546 (1989).
- [22] M. P. A. Fisher, G. Grinstein, and S. M. Girvin, Presence of quantum diffusion in two dimensions: Universal resistance at the superconductor-insulator transition, *Phys. Rev. Lett.* **64**, 587 (1990).
- [23] A. B. Harris, Effect of random defects on the critical behaviour of ising models, *Journal of Physics C: Solid State Physics* **7**, 1671 (1974).
- [24] J. T. Chayes, L. Chayes, D. S. Fisher, and T. Spencer, Finite-size scaling and correlation lengths for disordered systems, *Phys. Rev. Lett.* **57**, 2999 (1986).
- [25] M.-C. Cha, M. P. A. Fisher, S. M. Girvin, M. Wallin, and A. P. Young, Universal conductivity of two-dimensional films at the superconductor-insulator transition, *Phys. Rev. B* **44**, 6883 (1991).
- [26] K. Damle and S. Sachdev, Nonzero-temperature transport near quantum critical points, *Phys. Rev. B* **56**, 8714 (1997), [arXiv:cond-mat/9705206 \[cond-mat.str-el\]](#).
- [27] S. Sachdev, Nonzero-temperature transport near fractional quantum Hall critical points, *Phys. Rev. B* **57**, 7157 (1998), [arXiv:cond-mat/9709243 \[cond-mat.mes-hall\]](#).
- [28] X.-Y. Song, Y.-H. Zhang, and T. Senthil, Phase transitions out of quantum Hall states in moiré materials, *Phys. Rev. B* **109**, 085143 (2024), [arXiv:2308.10903 \[cond-mat.str-el\]](#).
- [29] C. L. Kane, M. P. A. Fisher, and J. Polchinski, Randomness at the edge: Theory of quantum Hall transport at filling $\nu=2/3$, *Phys. Rev. Lett.* **72**, 4129 (1994), [arXiv:cond-mat/9402108 \[cond-mat\]](#).
- [30] C. L. Kane and M. P. A. Fisher, Impurity scattering and transport of fractional quantum Hall edge states, *Phys. Rev. B* **51**, 13449 (1995), [arXiv:cond-mat/9409028 \[cond-mat\]](#).
- [31] C. L. Kane and M. P. A. Fisher, Contacts and edge-state equilibration in the fractional quantum Hall effect, *Phys. Rev. B* **52**, 17393 (1995), [arXiv:cond-mat/9506116 \[cond-mat\]](#).
- [32] C. de C. Chamon and E. Fradkin, Distinct universal conductances in tunneling to quantum hall states: The role of contacts, *Phys. Rev. B* **56**, 1212 (1997).
- [33] A. Young, Private communication (2024).
- [34] H. Park, Private communication (2025).
- [35] J. K. Jain, Composite-fermion approach for the fractional quantum hall effect, *Phys. Rev. Lett.* **63**, 199 (1989).
- [36] H. Goldman, A. P. Reddy, N. Paul, and L. Fu, Zero-Field Composite Fermi Liquid in Twisted Semiconductor Bilayers, *Phys. Rev. Lett.* **131**, 136501 (2023), [arXiv:2306.02513 \[cond-mat.mes-hall\]](#).
- [37] J. Dong, J. Wang, P. J. Ledwith, A. Vishwanath, and D. E. Parker, Composite Fermi Liquid at Zero Magnetic Field in Twisted MoTe₂, *Phys. Rev. Lett.* **131**, 136502 (2023), [arXiv:2306.01719 \[cond-mat.str-el\]](#).
- [38] L. Saminadayar, D. Glatthli, Y. Jin, and B. c.-m. Etienne, Observation of the $e/3$ fractionally charged laughlin quasiparticle, *Physical Review Letters* **79**, 2526 (1997).
- [39] R. De-Picciotto, M. Reznikov, M. Heiblum, V. Umansky, G. Bunin, and D. Mahalu, Direct observation of a fractional charge, *Physica B: Condensed Matter* **249**, 395 (1998).
- [40] J. Martin, S. Ilani, B. Verdene, J. Smet, V. Umansky, D. Mahalu, D. Schuh, G. Abstreiter, and A. Yacoby, Localization of fractionally charged quasi-particles, *Science* **305**, 980 (2004).

- [41] X.-Y. Song and T. Senthil, Density wave halo around anyons in fractional quantum anomalous hall states, *Physical Review B* **110**, 085120 (2024).
- [42] P. Nosov, Z. Han, and E. Khalaf (2025), to appear.
- [43] M. Cheng, S. Musser, A. Raz, N. Seiberg, and T. Senthil, Ordering the topological order in the fractional quantum Hall effect, [arXiv e-prints](#) , [arXiv:2505.14767](#) (2025), [arXiv:2505.14767 \[cond-mat.str-el\]](#).

Appendix A: Connection between the transitions out of bosonic/fermionic Jain states

In the main text, we analyzed various possible paths from the fermionic Jain state at $\nu = 2/3$ to a chiral topological superconductor with $c_- = -2$ by doping in the $a_{2/3}$ anyon. In this section, we provide an alternative perspective on these transitions by relating the fermionic Jain state to a bosonic Jain state of charge-2 Cooper pairs at the same filling stacked with a fermionic integer quantum Hall state. The possibility of such a mapping is due to the fact that powers of $a_{2/3}$ cannot generate the physical electron. As a result, the low energy Hilbert space is bosonic and various transitions admit a purely bosonic description. In this Appendix, we will develop this description which will give an interesting alternate theoretical viewpoint on the FQAH-SC evolution described in the main text.

The fermionic $2/3$ Jain state has Hall conductivity $\sigma_{xy}^f = 2e^2/3h$ and a chiral central charge $c_-^f = 0$. The 3 distinct anyons generated by $a_{2/3}$ are $(1, a_{2/3}, a_{2/3}^2)$ which have statistics $(0, 2\pi/3, 2\pi/3) \bmod 2\pi$ respectively. The corresponding electric charges are $0, 2/3, 4/3$. These anyons form a complete *bosonic* topological order by themselves (which we denote $\mathcal{V}^{2,3}$). The full anyon content of the fermionic $2/3$ Jain state can be described as the tensor product $\mathcal{V}^{2,3} \times (1, c)$ where c is the physical electron.

Consider now a different theory, namely, the bosonic $2/3$ Jain state of charge-2 Cooper pairs⁶. This has electrical Hall conductivity $\sigma_{xy}^b = 8e^2/3h$, and a chiral central charge $c_-^b = 2$. Following standard arguments, this will have a vison v (the anyon nucleated by 2π flux threading) with statistics $2\pi/3$ and electric charge $8/3$. The full topological order has 3 anyons $(1, v, v^2)$ with statistics $(0, 2\pi/3, 2\pi/3) \bmod 2\pi$ respectively. The corresponding electric charges are $(0, 8/3, 16/3) \simeq (0, 2/3, 4/3) \bmod 2$. The modding by 2 corresponds to binding Cooper pairs to get topologically equivalent particles.

Thus the anyon data of the bosonic Jain state exactly match that of $\mathcal{V}^{2,3}$ but the electrical conductivity and chiral central charge differ from the fermionic $2/3$ Jain state: $\sigma_{xy}^f = \sigma_{xy}^b - 2e^2/h$, $c_-^f = c_-^b - 2$. But this difference is precisely that of a $\sigma^{xy} = -2$ fermionic integer quantum Hall state. Thus we can view the fermionic $2/3$ Jain state as a bosonic $2/3$ Jain state of charge-2 Cooper pairs stacked with a $\nu = -2$ fermionic integer quantum Hall state. For other similar identifications, see the recent discussion in Ref. [43].

We can also obtain the same conclusion through an explicit field theoretic construction. Let us begin by considering a microscopic system of charge-2 bosons Φ at lattice filling $2/3$. To describe the bosonic Jain state, we consider a parton decomposition $\Phi = f_1 f_2$ and introduce an emergent $U(1)$ gauge field a to remove the gauge redundancy. The parton Lagrangian takes the form

$$L[\Phi, 2A] = L[f_1, 2A - a] + L[f_2, a]. \quad (\text{A1})$$

We interpret the charge-2 boson as the bound state of two physical fermions, each carrying charge 1. In this case, A, a are spin_C connections and $2A$ is an ordinary $U(1)$ gauge field. At the mean-field level, we choose the flux of a to be proportional to $2\pi/3$ so that f_1, f_2 can form Chern insulators with Chern numbers C_1, C_2 . To construct the bosonic Jain state, we take $C_1 = 2, C_2 = 1$. Integrating out the gapped f_1, f_2 then produces an effective Lagrangian

$$L_{\text{bosonic}, 2/3} = \frac{2}{4\pi}(2A - a)d(2A - a) + \frac{1}{4\pi}ada + 6\text{CS}_g. \quad (\text{A2})$$

Now we make a change of variables $a = b + A$ so that b is an ordinary $U(1)$ gauge field. The resulting Lagrangian simplifies to

$$L_{\text{bosonic}, 2/3} = \frac{2}{4\pi}(A - b)d(A - b) + \frac{1}{4\pi}(b + A)d(b + A) + 6\text{CS}_g = \frac{3}{4\pi}bdb - \frac{1}{2\pi}bdA + \frac{3}{4\pi}AdA + 6\text{CS}_g. \quad (\text{A3})$$

The difference between this Lagrangian and the Lagrangian in (3) for the fermionic Jain state is precisely the response theory for a $\nu = -2$ fermionic IQH state. We therefore conclude that

$$L_{\text{fermionic}, 2/3} = L_{\text{bosonic}, 2/3} - \frac{2}{4\pi}AdA - 4\text{CS}_g. \quad (\text{A4})$$

The above matches the topological order and the charge assignments of the fermionic $2/3$ Jain state and the bosonic one stacked with a $\nu = -2$ fermion IQHE. The projective translation symmetry action on the anyons will also be the same. This is because at lattice filling $2/3$, there will be a background anyon in each unit cell which is the charge $2/3$

⁶ In a Landau level setting this will be described as the Halperin $(2, 2, 1)$ state. The corresponding 2×2 K -matrix has $K_{11} =$

$K_{22} = 2, K_{12} = K_{21} = 1$ and a charge vector $(2, 2)$.

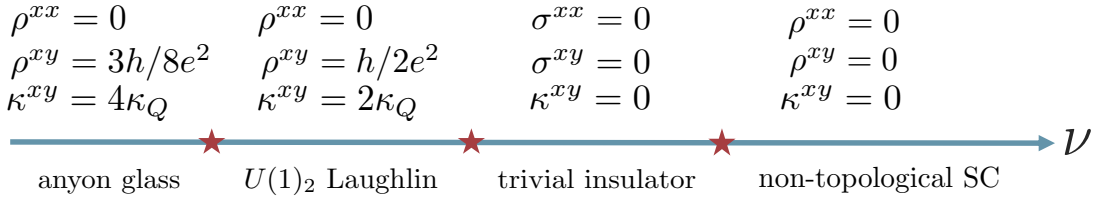


FIG. 7. Phase diagram of the doped bosonic Jain state in the dirty limit with short-wavelength disorder. Note that the four phases here can be obtained from the four phases in Fig. 4 by stacking with a $\nu = -2$ fermionic IQH state.

anyon. The translation symmetry action on any anyon is completely determined by its braiding phase around the background anyon, which in turn is determined by its fractional charge. Since we have already matched the charges, the translation action will also match.

Within the bosonic theory, doping the $a_{2/3}$ anyon corresponds to doping into the f_1 band. When the disorder potential has large short-wavelength modulations, the evolution from the bosonic Jain state to the trivial superconductor passes through four stages, in which the Hall conductance of f_1 is $\sigma_{f_1}^{xy} = 2, 1, 0, -1$ respectively. When $\sigma_{f_1}^{xy} = 2$, we recover the bosonic Jain state at $\nu = 2/3$. When $\sigma_{f_1}^{xy} = 1$, we obtain

$$L = \frac{1}{4\pi}(2A - a)d(2A - a) + \frac{1}{4\pi}ada + 4CS_g. \quad (A5)$$

We recognize this Lagrangian as the standard parton description of the bosonic $U(1)_2$ state with charge-2 bosons. When $\sigma_{f_1}^{xy} = 0$, the Lagrangian reduces to

$$L = \frac{1}{4\pi}ada + 2CS_g, \quad (A6)$$

which describes a trivial insulator. Finally, when $\sigma_{f_1}^{xy} = -1$, we can again make a change of variables $a = b + A$ to get an effective theory

$$L_{\text{bosonic}, 2/3}[A] = -\frac{1}{4\pi}(A - b)d(A - b) + \frac{1}{4\pi}(b + A)d(b + A) = \frac{2}{2\pi}bdA. \quad (A7)$$

Therefore, the bosonic sector describes a trivial charge-2 superconductor. This four-stage evolution is summarized in Fig. 7. In the clean limit (or with smooth disorder), two of these intermediate phases with $\sigma_{f_1}^{xy} = 1$ and $\sigma_{f_1}^{xy} = 0$ disappear and we are left with a direct transition between the bosonic Jain state and the trivial charge-2 superconductor.

As a sanity check, we can verify that the four phases (see Fig. 4) in the doped fermionic Jain state can be directly obtained from the four phases (see Fig. 7) in the doped bosonic Jain state by stacking with a $\nu = -2$ integer quantum Hall state of electrons. This is of course consistent with the relation in (A4).

Since the background $\nu = -2$ integer quantum Hall response does not influence the dynamics of the system, the transitions between neighboring phases in Fig. 4 lie in the same universality class as the corresponding transitions in Fig. 7. This observation provides additional insight into the nature of these transitions. For example, the transition between the $U(1)_{-2}$ neutral topological order and the $\nu = -2$ IQH state in the fermionic formulation is mapped to a transition between the $U(1)_2$ bosonic Laughlin state and a trivial insulator. The latter transition admits a simple Chern-Simons description in the clean limit, which can be studied numerically in the presence of disorder. Similarly, the transition between the $\nu = -2$ IQH state and the chiral topological SC in the fermionic formulation is mapped to a standard superfluid-insulator transition in the bosonic formulation, about which a lot of progress has been made since the pioneering works of Refs. [21, 22].

Finally, in a clean system, after removing the stacked IQH states, the bandwidth tuned fermionic $2/3$ Jain-chiral topological SC gets exactly related to the bosonic $2/3$ Jain to the trivial SC transition. This latter transition is part of the family of bosonic $p/(p+1)$ Jain - trivial SC transitions which are described by $p+1$ massless Dirac fermions coupled to a $U(1)$ gauge field with a Chern-Simons action:

$$L_{\text{DiracB}} = \sum_{I=1}^{p+1} d_I^\dagger (i\vec{\partial} + \vec{\phi}) d_I + \frac{p+1}{4\pi}ada - \frac{2}{2\pi}adA + \frac{4}{4\pi}AdA + 2(p+1)CS_g. \quad (A8)$$

(We have assumed that the physical bosons have charge-2). Setting $p = 2$, and letting $a = A - b$, we see that we recover Eqn. 22 after removing the $\nu = 2$ fermionic IQH response.

Appendix B: Transport in a Boltzmann gas of charged anyons

In this section, we provide a semiclassical modeling of the transport properties of a thermal gas of charge- q anyons in the Boltzmann regime. When the number density of anyons is δ , the degeneracy temperature is on the order of δ/m where m is the anyon effective mass. Boltzmann transport applies whenever $T \gg \delta/m$. If the anyon gas originates from doping a FQAH state, then δ is the mobile dopant charge density. An additional upper bound $T \ll \Delta_{\text{Jain}}$ is required so that the basic physics responsible for the formation of the anyons is not destroyed by thermal fluctuations. Therefore, we impose the more stringent criterion

$$\frac{\delta}{m} \ll T \ll \Delta_{\text{Jain}}. \quad (\text{B1})$$

When the above condition is satisfied, we can write down the semiclassical equations of motion for a single charged anyon in the presence of an applied electric field \mathbf{E} and magnetic field \mathbf{B} in the absence of any scattering

$$\frac{d\mathbf{x}}{dt} = \frac{\mathbf{p}}{m} - \frac{d\mathbf{p}}{dt} \times \Omega \hat{z}, \quad \frac{d\mathbf{p}}{dt} = q \left(\mathbf{E} + \frac{d\mathbf{x}}{dt} \times \mathbf{B} \right). \quad (\text{B2})$$

In this equation, Ω is an effective Berry curvature which is generically nonzero in a system with broken time-reversal symmetry. In a classical Hamiltonian system, this Berry curvature arises from a nontrivial Poisson bracket $\{x, y\} = \Omega$ which modifies the symplectic structure on the phase space defined by (x, y, p_x, p_y) . Since the precise value of Ω does not play an important role in our argument, we will leave it as a phenomenological parameter. To linear order in \mathbf{E} and \mathbf{B} , these equations become

$$\frac{d\mathbf{x}}{dt} = \frac{\mathbf{p}}{m} - q\mathbf{E} \times \Omega \hat{z}, \quad \frac{d\mathbf{p}}{dt} = q \left(\mathbf{E} + \frac{d\mathbf{x}}{dt} \times \mathbf{B} \right). \quad (\text{B3})$$

Introducing momentum relaxation at a time scale τ , the second equation becomes

$$\frac{d\mathbf{p}}{dt} = -\frac{\mathbf{p}}{\tau} + q \left(\mathbf{E} + \frac{d\mathbf{x}}{dt} \times \mathbf{B} \right) \quad (\text{B4})$$

Solving these equations in the DC limit, we obtain the total conductivity from the anyon gas sector

$$\sigma = \begin{pmatrix} \sigma_0 & \sigma_{\text{anom}} + \sigma_{\text{conv}}(B) \\ -\sigma_{\text{anom}} - \sigma_{\text{conv}}(B) & \sigma_0 \end{pmatrix}, \quad (\text{B5})$$

where

$$\sigma_0 = \frac{\delta q^2 \tau}{m [1 + (\omega_c \tau)^2]}, \quad \sigma_{\text{anom}} = -\delta q^2 \Omega, \quad \sigma_{\text{conv}}(B) = \sigma_0 \omega_c \tau, \quad \omega_c = qB/m. \quad (\text{B6})$$

To get the full conductivity, we need to add the contribution from the $\nu = 2/3$ Jain state:

$$\sigma_c = \begin{pmatrix} \sigma_0 & \sigma_{\text{anom}} + \sigma_{\text{conv}}(B) + 2e^2/3h \\ -\sigma_{\text{anom}} - \sigma_{\text{conv}}(B) - 2e^2/3h & \sigma_0 \end{pmatrix}. \quad (\text{B7})$$

Since σ_0 is a constant up to $\mathcal{O}(B^2)$ corrections at small B , we know that

$$\left. \frac{d\sigma^{xy}}{dB} \right|_{B=0} = \frac{\delta q^2 \tau}{m} \frac{q\tau}{m}. \quad (\text{B8})$$

Dividing by the longitudinal conductance then gives

$$\frac{1}{(\sigma^{xx})^2} \left. \frac{d\sigma^{xy}}{dB} \right|_{B=0} = \frac{\delta q^3 \tau^2}{m^2} \frac{m^2}{\delta^2 q^4 \tau^2} = \frac{1}{\delta q}. \quad (\text{B9})$$

This allows us to infer the mobile carrier density δ .